INVESTIGACIÓN E INNOVACIÓN EN INGENIERÍAS

Feasibility of Polarization Division Multiplexing for Bidirectional Optical Links in 5G Radio over Fiber Cloud Access Networks

Viabilidad del Multiplexado por División de Polarización para Enlaces Ópticos Bidireccionales en Redes de Acceso en la Nube Radio sobre Fibra 5G

Gustavo Adolfo Puerto Leguizamón
Carlos Arturo Suárez Fajardo
Universidad Distrital Francisco José de Caldas, Colombia

OPEN ACCESS

Recibido:
24/07/2024
Aceptado:
30/09/2024
Publicado:
16/12/2024

Correspondencia:
gapuerto@udistrital.edu.co

DOI:
https://doi.org/10.17081/invinno.12.2.7250

Abstract
Objective: To investigate the potential of polarization division multiplexing in a 5G radio over fiber cloud access network to enable bidirectional optical links in the front-haul segment. **Methodology:** An optically centralized cloud radio access network based on polarization division multiplexing and radio-over-fiber transport is proposed. The exploitation of the polarization domain enables independent optical wavelength channels for the downlink and uplink. The experimental demonstration assesses the feasibility of the radio-over-fiber transport of information in a 5G-cloud radio access network. The demonstration evaluated the Error Vector Magnitude measurements for optical carrier linewidths of 0.1 nm. Data was experimentally measured for QPSK and 64QAM signals onto 3.5 GHz radio frequency across 10 km and 20 km of single mode optical fiber. **Results:** The experimental results evaluated the quality of the QPSK and 64QAM signals transported onto a polarization division multiplexing environment for an optically centralized transport in a 5G-cloud radio access network. 64QAM featured an EVM below 6% with a degradation of 2.8% and QPSK presented and EVM below 8% with a degradation of roughly 4.8% with respect to the back-to-back signal across a propagation length of 20 km. **Conclusions:** The results demonstrated that polarization multiplexing for an optically centralized transport in a 5G-cloud radio access network is feasible. Despite the relatively low optical power received in the uplink, the power penalties of the polarized components did not compromise the power budget so that optical amplification was not included in the measurements. Both QPSK and 64QAM fulfills the requirements of the 3GPP in terms of quality and signal integrity.

Keywords: Polarization Division Multiplexing, 5G Radio-over-Fiber, Cloud Radio Access Network, Bidirectional optical links, Front-haul segment, Error Vector Magnitude.

Resumen
Objetivo: Investigar el potencial de la multiplexación por división de polarización en una red de acceso radio sobre fibra en la nube para 5G con el fin de habilitar enlaces ópticos bidireccionales en el segmento de front-haul. **Metodología:** Se propone una red de acceso de radio en la nube ópticamente centralizada basada en multiplexación por división de polarización y transporte de radio sobre fibra. La explotación del dominio de polarización genera canales de longitud de onda óptica independientes para el enlace descendente y el enlace ascendente. La demostración experimental evalúa la viabilidad del transporte de información por radio sobre fibra en una red de acceso de radio en la nube 5G. La demostración evaluó las mediciones de la magnitud del vector de error para anchos de línea de portadoras ópticos de 0.1 nm. Los datos se midieron experimentalmente para señales QPSK y 64QAM sobre una radiofrecuencia de 3.5 GHz a lo largo de 10 km y 20 km de fibra óptica monomodo. **Resultados:** Los resultados experimentales evaluaron la calidad de las señales QPSK y 64QAM transportadas en un entorno de multiplexación por división de polarización para un transporte ópticamente centralizado en una red de acceso de radio en la nube para 5G. 64QAM presentó un EVM por debajo del 6% con una degradación del 2.8% y QPSK presentó un EVM por debajo del 8% con una degradación de aproximadamente el 4.8% con respecto a la señal original a lo largo de una longitud de propagación de 20 km. **Conclusiones:** Los resultados demostraron que la multiplexación de polarización para un transporte ópticamente centralizado en una red de acceso de radio en la nube para 5G es factible. A pesar de la potencia óptica relativamente baja recibida en el enlace ascendente, las penalizaciones de potencia de los componentes polarizados no comprometieron el presupuesto de potencia, por lo que la amplificación óptica no se incluyó en las mediciones. Tanto QPSK como 64QAM cumplen los requisitos del 3GPP en términos de calidad e integridad de la señal.

Palabras claves: Multiplexación por División de Polarización, Radio-sobre-Fibra 5G, Red de Acceso Radio en la Nube, Enlaces ópticos bidireccionales, segmento Front-haul, Magnitud del Vector de Error.

Como citar (IEEE): G.A. Puerto Leguizamón, C.A. Suárez Fajardo "Feasibility of Polarization Division Multiplexing for Bidirectional Optical Links in 5G Radio over Fiber Cloud Access Networks", Investigación e Innovación en Ingenierías, vol. 12, no. 2, pp. 218–227, 2024, doi: https://doi.org/10.17081/invinno.12.2.7250

Introduction

The vision for 5G wireless networks and beyond revolves around the promise of incredibly fast speeds, seamless connectivity and revolutionary applications that demand ultra-low latency, high bandwidth and low power consumption [1]. To realize this vision, a fundamental shift in the network architecture is required. Radio-over-Fiber (RoF) technology emerges as a crucial bridge between wireless and optical communications that offers a robust solution to many of the challenges posed by 5G [2]. The capability of RoF to transmit high-bandwidth, low-latency signals over fiber optic links positions it as an important component of the fronthaul. The fronthaul segment of the 5G network links the Distributed Unit (DU) with the Radio Units (RUs) [3]. In this context, the fronthaul links, DUs and RUs, among others, are elements that constitute the Cloud-Radio Access Network (C-RAN), in which the Common Public Radio Interface (CPRI) and Digital Radio transport the data over Fiber.

However, there are growing concerns regarding the effectiveness of this solution nowadays [4]. The capacity of fronthaul based on CPRI is directly related to the radio bandwidth, the quantity of antenna elements and the sectors of the RU [5,6]. This fact requires improvements in the optical segment, which initially led to deploy optical fronthaul interfaces at 25 Gb/s, exemplified by CPRI option 10 line rate [5] and compatible transceivers [7,8,9]. Conversely, the enhanced CPRI (eCPRI) promotes higher-layer functional splits to alleviate the ever-growing demand for data rates over the optical interface at the expenses of requiring more intricate RU setups [10,11]. Furthermore, the emerging 5G Frequency Range 2 (FR-2) above 24 GHz is expected to leverage extensive capacities, massive Multiple Input Multiple Output (m-MIMO) configurations, and beamforming [12], which poses a challenge for existing commercial solutions in terms of unsustainable bitrate scaling [13,14].

Therefore, the way optical carriers are managed to transport radio signals significantly impacts both performance and operational cost within the C-RAN. In this context, Polarization Division Multiplexing (PDM) stands as a novel technique for the transport of information, particularly in optical communication systems. By exploiting the orthogonal polarization states of lightwaves, PDM allows for the simultaneous transmission of multiple streams of data over a single optical fiber. This technique aims at effectively enable a higher data-carrying capacity of the fiber without requiring additional physical infrastructure and ensures that the fronthaul links can accommodate the massive amounts of data generated by multiple RUs, enhancing network flexibility, scalability, and spectral efficiency.

Thus, through carefully management of the polarization states of lightwaves at the transmitter side and the receiver end, PDM has shown efficient and robust data transmission in the fronthaul, as presented in [15,16]. Also, fixed-mobile converged transport [17] as well as Free Space Optics (FSO)-5G convergence [18] based on PDM have been demonstrated. Moreover, the impact of PDM in terms of spectral efficiency in high-speed optical communication networks has been presented in [19,20,21]. Furthermore, as data demands continue to increase, several proposals have demonstrated that PDM is a promising approach to meet the ever-growing need for higher bandwidth and enhanced data throughput in wireless communication systems operating in millimeter waves (MMW) [22,23,24].

In this work, the analysis and performance of a centralized C-RAN based on PMD and RoF transport is presented. The optical centralized feature of this approach implies the placement of optical lasers only in the DU side avoiding the use of optical active components in the RUs. This fact leads to reduce the complexity and energy consumption at the RUs side. Then, PDM enables bidirectional transmission as one of the orthogonal components is used in the downlink and the other orthogonal component is used in the uplink. The conducted experiments measured the Error Vector Magnitude (EVM) of service profiles transported in Quadrature Phase Shift Keying (QPSK) and 64 Quadrature Amplitude Modulation (64QAM) modulation formats.

Unlike the previous works, this proposal demonstrates the use of PDM in C-RAN in order to enable optical links for the transport of information between DUs and RUs and vice versa. This characteristic enables profitable and low power consumption RoF transport of signals covering the typical distances of a 5G C-RAN. The paper is organized as follows: section II analytically describes the approach and presents the experimental implementation. Section III describes the experimental results of the proposed approach and section IV summaries the paper.

Methodology

Detailed methodological stages that include both mathematical descriptions and an experimental setup were followed in order to develop the proposed approach. In this context, the methodological stages comprise (a) a mathematical description of the polarization multiplexing and demultiplexing technique, (b) the design of the optical network that includes operation frequency, bandwidth and modulation format used to assess the proposal. This section describes the methodological stages used in this work.

Analytical description of the optically centralized C-RAN

PDM is based on the use of Polarization Beam Splitters (PBS) and Polarization Beam Combiners (PBC). These two devices are respectively in charge of separating the orthogonal components of the lightwave electrical field and combine them again once they have been modulated or processed as needed. In our approach, xPol is used to modulate the downlink signal, i.e. the information signal from the DU to the RU. Similarly, yPol is the unmodulated component that is launched from the DU to the RU in order to enable the optical transmission in the uplink, i.e. the transmission from the RU to the DU. Regarding the polarization treatment of the signal, an arbitrary state of polarization of an electrical field can be split up as an addition of two orthogonal states of polarization. The envelope of such electric field is described by:

$$E = E_{xPol}\hat{x} + E_{yPol}\hat{y} = a_x e^{j\varphi_x}\hat{x} + a_y e^{j\varphi_y}\hat{y} \quad (1)$$

Where $\hat{\mathbf{x}}$ and $\hat{\mathbf{y}}$ represent the unit vectors in *x* direction and *y* direction respectively. Then, the two components Jones vector can express any polarization state as:

$$J = \begin{pmatrix} E_{xPol} \\ E_{yPol} \end{pmatrix} = \begin{pmatrix} a_x e^{j\varphi_x} \\ a_y e^{j\varphi_y} \end{pmatrix} \quad (2)$$

In such a context, if J_i and J_o are respectively the Jones vectors of the polarization states at the input and output of the polarization beam splitter, the Jones matrix *M* that relates inputs and outputs of such device is given by:

$$M = \begin{pmatrix} 1 & 0 \\ 0 & 0 \end{pmatrix} + \begin{pmatrix} 0 & 0 \\ 0 & 1 \end{pmatrix} \quad (3)$$

The first and second addends represent the Jones matrix of the horizontal polarization state and vertical polarization state respectively. Since $\mathbf{J_o} = \mathbf{M} \cdot \mathbf{J_i}$, the output of the polarization beam splitter based on (2) and (3) is expressed as:

$$\begin{pmatrix} E^o_{xPol} \\ E^o_{yPol} \end{pmatrix} = \begin{pmatrix} 1 & 0 \\ 0 & 0 \end{pmatrix} \cdot \begin{pmatrix} E^i_{xPol} \\ E^i_{yPol} \end{pmatrix} + \begin{pmatrix} 0 & 0 \\ 0 & 1 \end{pmatrix} \cdot \begin{pmatrix} E^i_{xPol} \\ E^i_{yPol} \end{pmatrix} \quad (4)$$

Thus, the orthogonal component in which the information is transported in the downlink (xPol) is represented by the first addend. The second addend (yPol), represents the unmodulated component that will be used in the uplink. In this way, the C-RAN is optically centralized since it is not necessary to place optical sources in the RUs.

Implementation details

Figure 1 shows the layout of the experimental setup. The optical comb generator is based on optical filtering and a broadband optical source as described in [25]. In this context, the optical comb generator produces optical carriers featuring a

linewidth of 0.1 nm in C band. Then, the PBS separates the optical carrier into two orthogonal polarized signals, xPol and yPol. The former polarized component is used to feed an electro-optic modulator (EOM) that receives the information signals of the arbitrary waveform generator (AWG) and the later keeps unmodulated since it will be used for the uplink transmission. It should be pointed out that Frequency Range 1 (FR-1) band of 5G is included in the evaluated radio frequency bandwidth; in particular, 25Mbauds on 64QAM was modulated onto 3.5 GHz in the downlink.

Subsequently, both orthogonal channels are multiplexed in the polarization beam combiner (PBC) and launched through the Optical Circulator 1 (OC1) to the optical Single Mode Fiber (SMF) link. The performance was assessed under various propagation conditions by testing the system over different link lengths that included optical links of 10 km and 20 km. Next, after RoF signals propagation through the fiber, the Optical Circulator 2 (OC2) sends the received signal to the PBS in order to demultiplex both polarized components. Then, an optical receiver was used to convert the xPol signal back into an electrical signal to assess the downlink system performance in the AWG.

Next, the unmodulated yPol feeds the EOM to constitute the uplink optical channel that consists of 15Mbauds QPSK modulated onto 3.5 GHz. In this context, the uplink signal is sent to the optical link through OC2, after fiber propagation OC1 directs the uplink transmission to the respective optical receiver, which detects the incoming signal, performs optical-to-electrical conversion and sends the received electrical signal to the AWG for the evaluation of the signal quality.

Figure 1. Experimental setup for the optically centralized C-RAN based on PDM

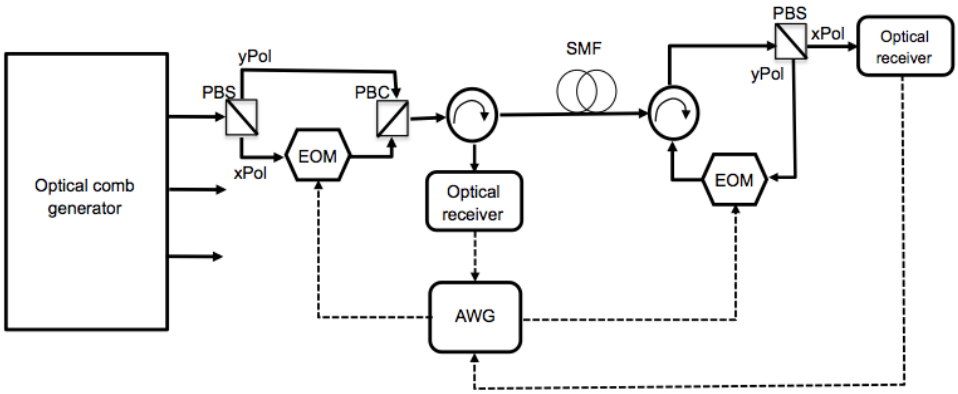

Source: Own Elaboration

Results

Figure 2 shows the spectra of the polarized optical carriers measured at different points of the proposed layout. In particular, the spectra of the downlink are observed for xPol and yPol components in both the transmitter and receiver end. As observed, xPol carries the downlink information while yPol is transmitted without data signal. The optical power difference between the transmitted signal and the received one corresponds to the insertion losses of the link that account for roughly 6 dB and includes the PBC, the circulators, 20 km of optical fiber and the PBS. Both xPol and yPol underwent the same power penalty resulting in an optical receiver power of -16 dB. Then, yPol was fed to the EOM to enable uplink optical modulation whose transmitted and received optical spectrum is shown in the bottom row of Figure 2. Overall, the received optical power in the uplink was -25 dB.

Figure 2. Experimental results. Downlink and uplink signals in the centralized C-RAN

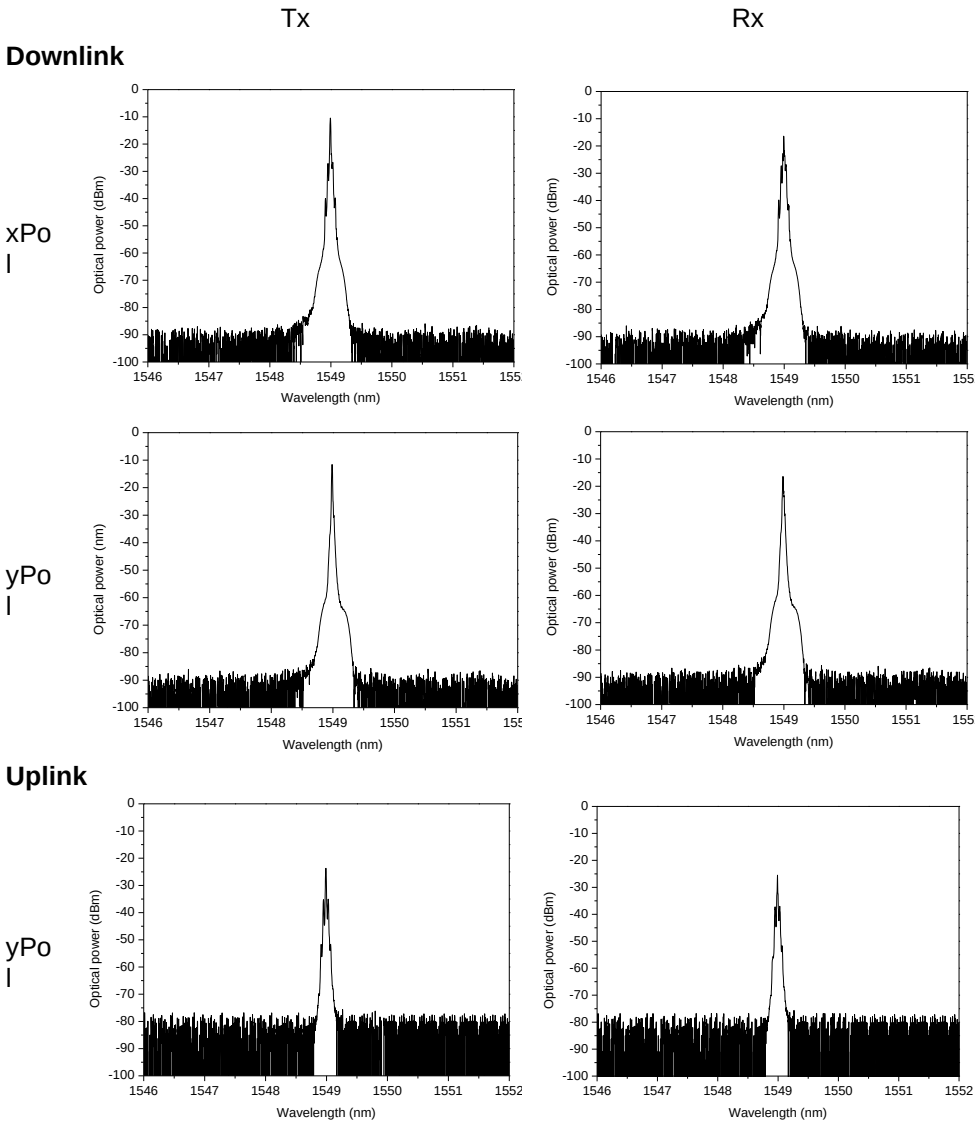

Source: Own Elaboration

The constellations of the downlink and uplink after a fiber propagation of radio signals across 10 km and 20 km are shown in Figure 3. In particular, Figure 3(a) represents the 64QAM downlink signal after 10 km and Figure 3(b) shows the constellation of the downlink signal after a fiber spam of 20 km. The measured EVM of the downlink after 10 km was 4% and 6.2% was found for a propagation length of 20 km. Regarding the uplink, Figure 3(c) and Figure 3(d) shows the constellation of the received QPSK signal after 10 km and 20 km respectively. In this context, the measured EVM of the uplink was 8% after 10 km and 10.1% after 20 km of fiber propagation.

Figure 3. Experimental results. Measured constellations of the downlink and uplink signals in the centralized C-RAN

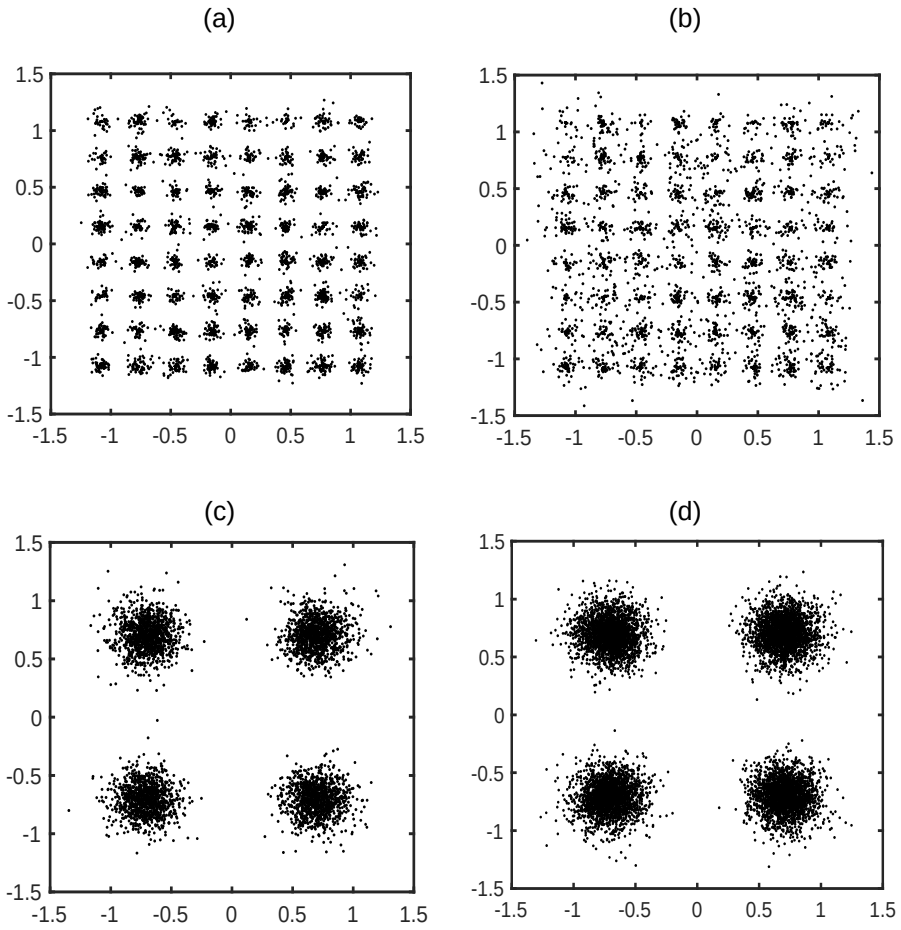

Source: Own Elaboration

The signal degradation for the downlink and uplink was measured for QPSK and 64QAM modulation formats. Figure 4 shows the quality of the downlink services on a fiber spam of 10 km for the 64QAM signal, the results show an EVM below 4% for received optical powers above -16 dBm and with a degradation of roughly 0.7% compared to the back-to-back value. The obtained results for a fiber link of 20 km show an EVM below 6% for optical powers above -16dBm featuring a degradation of 2.8% with respect to the back-to-back result. It is noticeable the increasing degradation as the optical power is reduced. In this context, the third Generation Partnership Project (3GPP) defined the maximum EVM values for 5G standard according to the modulation format deployed [26]. Thus, the EVM limit for a 64QAM modulation is 8% and it is represented with dashed lines in Figure 4. Therefore, in accordance with this requirement, whilst the EVM limit for a downlink featuring 10 km of fiber propagation is found when the received optical power in -20.5 dBm, the EVM limit for a downlink propagation of 20 km is fulfilled for received optical powers below -18 dBm.

Similarly, the experimental results showing the quality of the uplink QPSK signal are shown in Fig. 5. The results show an EVM below 8% for received optical powers above -25 dBm and with a degradation of roughly 4.8% compared to the back-to-back. Such results were found for an uplink length of 10 km. For an uplink length of 20 km, an EVM below 10% was found for optical powers above -25 dBm, this

represents a degradation of 6.8% with respect to the back-to-back result. As far as the EVM limit for QPSK signals is concerned, 3GPP set a maximum EVM of 17.5% for QPSK modulation format, in our approach this limit is found for a fiber length of 10 km with a received optical power of -31dBm. For a 20 km fiber spam the EVM limit is found with a received power of -29 dBm.

Figure 4. Experimental results. Measured constellations of the downlink and uplink signals in the centralized C-RAN

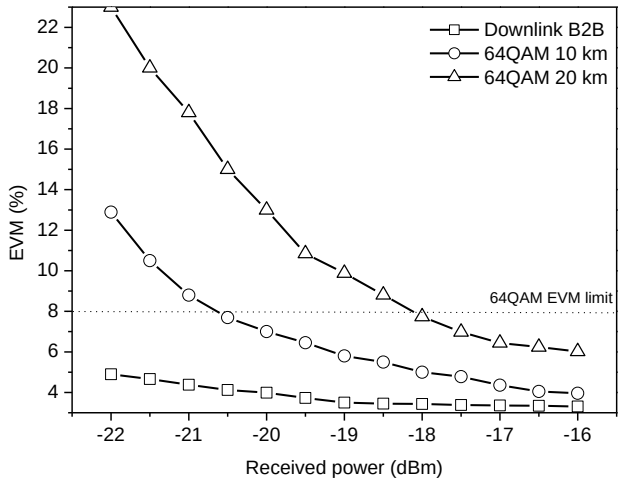

Source: Own Elaboration

Figure 5. Experimental results. Measured constellations of the downlink and uplink signals in the centralized C-RAN

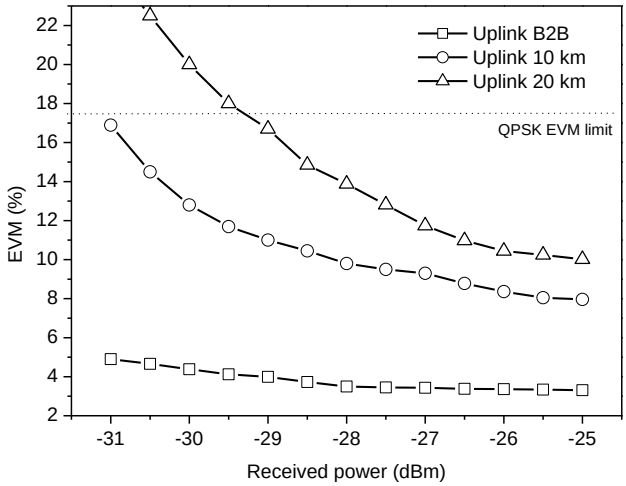

Source: Own Elaboration

Conclusion

This paper presented and demonstrated a proposal for an optically centralized 5G C-RAN based on PDM and RoF transport. The approach aims at providing a solution for the transport of services in the front-haul of a C-RAN deployment in order to reduce the complexity and energy consumption at the RUs side. Bidirectional transmission of RoF signals was demonstrated by exploiting the polarization domain of a lightwave.

The conducted measurements characterized the spectra of both polarization components transmitted across fiber spams of 10 km and 20 km, which represent

typical distances of a front-haul segment of a C-RAN. In this context, xPol transported the RoF signals in the downlink and yPol transported the RoF signals in the uplink. The evaluated RoF signals consisted of QPSK and 64QAM modulation formats onto 3.5 GHz; this frequency belongs to the FR-1 band of 5G. The obtained results confirmed that QPSK and 64QAM satisfy the EVM requirement within the assessed fiber links. Negligible penalties due to chromatic dispersion were found due to the relatively narrow linewidth of the optical comb generator and the short length propagation.

EVM measurements for both modulation formats were performed and contrasted against the EVM limit defined by the 3GPP. In particular, we found that the EVM limit of 8% for a downlink conveying a 64QAM RoF signal onto 3.5 GHz propagated through 20 km is fulfilled for received optical powers above -18 dBm. On the other hand, the signal quality of the uplink transporting a QPSK RoF onto 3.5 GHz signal across 20 km featured an EVM limit of 17.5% with a received power of -29 dBm. Certainly, substantial differences concerning the received power were found particularly in the yPol component since it traveled twice the distance of the xPol component. However, the received power in the uplink, roughly -25.3 dBm, was in the sensitivity range of a typical PIN photo detector.

Overall, the outcomes shown in this paper demonstrates the feasibility of the approach in terms of the offered capacity and distance required for the deployment of current and next generation mobile networks. It is important to point out that the experimental results did not include optical amplification processes. By doing so, the capacity and reach of the proposed approach can be further improved.

Bibliographic References

[1] B. Agarwal, M. A. Togou, M. Marco and G. -M. Muntean, "A Comprehensive Survey on Radio Resource Management in 5G HetNets: Current Solutions, Future Trends and Open Issues," in IEEE Communications Surveys & Tutorials, vol. 24, no. 4, pp. 2495-2534, Fourthquarter 2022, doi: 10.1109/COMST.2022.3207967.

[2] J. Brenes et al., "Network slicing architecture for SDM and analog-radio-over-fiber-based 5G fronthaul networks," in Journal of Optical Communications and Networking, vol. 12, no. 4, pp. B33-B43, April 2020, doi: 10.1364/JOCN.381912.

[3] X. Liu, "Enabling Optical Network Technologies for 5G and Beyond," in Journal of Lightwave Technology, vol. 40, no. 2, pp. 358-367, 15 Jan.15, 2022, doi: 10.1109/JLT.2021.3099726.

[4] "IEEE Standard for Packet-based Fronthaul Transport Networks," in IEEE Std 1914.1-2019 , vol., no., pp.1-94, 21 April 2020, doi: 10.1109/IEEESTD.2020.9079731

[5] CPRI Specification V7.0 (2015-10-09). [Online] Available: http://www.cpri.info/downloads/CPRI_v_7_0_2015-10-09.pdf.

[6] S. Mikroulis, L. N. Binh, I. N. Cano and D. Hillerkuss, "CPRI for 5G Cloud RAN? – Efficient Implementations Enabling Massive MIMO Deployment – Challenges and Perspectives," 2018 European Conference on Optical Communication (ECOC), Rome, Italy, 2018, pp. 1-3, doi: 10.1109/ECOC.2018.8535213.

[7] X. Wang, "PAM-X™: A 25Gb/s-PAM4 Optical Transceiver Chipset for 5G Optical Front-Haul," OFC, M2F.6, San Diego, CA, USA, March 2020.

[8] H. Yu, et. al. "100Gbps CWDM4 Silicon Photonics Transmitter for 5G applications," OFC, W3E.4, San Diego, CA., USA, March 2019.

[9] P. Perry, A. Peters, S. McClean, P. Morrow, B. Scotney and L. Barry, "All-Optical Network Capacity for 5G Cellular Fronthaul," 2019 21st International Conference on Transparent Optical Networks (ICTON), Angers, France, 2019, pp. 1-4, doi: 10.1109/ICTON.2019.8840341.

[10] eCPRI specifications V2.0 (2019-05-10) [Online] Available: https://www.gigalight.com/downloads/standards/ecpri-specification.pdf

[11] C. S. Shinde, "A pragmatic industrial road map for shifting the existing fronthaul from CPRI to 5G compatible eCPRI," 2020 IEEE 3rd 5G World Forum (5GWF), Bangalore, India, 2020, pp. 297-302, doi: 10.1109/5GWF49715.2020.9221322.

[12] 3GPP TS 38.101–1: “New radio (NR): User equipment (UE) radio transmission and reception," V16.1.0, 2019.

[13] H. -H. Lu et al., "Two-Way 5G NR Fiber-Wireless Systems Using Single-Carrier Optical Modulation for Downstream and Phase Modulation Scheme for Upstream," in Journal of Lightwave Technology, vol. 41, no. 6, pp. 1749-1758, 15 March15, 2023, doi: 10.1109/JLT.2022.3230375.

[14] Y. Zhu and W. Hu, "Optical access networks for fixed and mobile applications [Invited Tutorial]," in Journal of Optical Communications and Networking, vol. 16, no. 2, pp. A118-A135, February 2024, doi: 10.1364/JOCN.499341.

[15] C. Li, X. Chen, Z. Chen and F. Zhang, "Capacity Increase in Dual-polarization Nonlinear Frequency Division Multiplexing Systems with Probabilistic Shaping," 2021 Opto-Electronics and Communications Conference (OECC), Hong Kong, Hong Kong, 2021, pp. 1-3, doi: 10.1364/OECC.2021.W1B.2.

[16] O. G. Morozov and A. M. Almufti, "Simulation with Investigation for 16Tbit/s High Order Quadrature Amplitude Modulation Dual Polarization Coherent Optical Transmission System for 5G and Beyond," 2023 Systems of Signal Synchronization, Generating and Processing in Telecommunications (SYNCHROINFO, Pskov, Russian Federation, 2023, pp. 1-5, doi: 10.1109/SYNCHROINFO57872.2023.10178497.

[17] S. Shen et al., "Polarization-Tracking-Free PDM Supporting Hybrid Digital-Analog Transport for Fixed-Mobile Systems," in IEEE Photonics Technology Letters, vol. 31, no. 1, pp. 54-57, 1 Jan.1, 2019, doi: 10.1109/LPT.2018.2882766

[18] H. -H. Lu et al., "Bi-Directional Fiber-FSO-5G MMW/ 5G New Radio Sub-THz Convergence," in Journal of Lightwave Technology, vol. 39, no. 22, pp. 7179-7190, 15 Nov.15, 2021, doi: 10.1109/JLT.2021.3113641

[19] M. Sun et al., "Spectrally Efficient Direct-Detection THz Communication System Enabled by Twin Single-Sideband Modulation and Polarization Division Multiplexing Techniques," 2022 Asia Communications and Photonics Conference (ACP), Shenzhen, China, 2022, pp. 53-56, doi: 10.1109/ACP55869.2022.10088517.

[20] Y. Cai et al., "Spectrally Efficient PDM-Twin-SSB Direct-Detection THz System Without Active Polarization Control," in IEEE Photonics Technology Letters, vol. 35, no. 15, pp. 838-841, 1 Aug.1, 2023, doi: 10.1109/LPT.2023.3275921.

[21] S. -A. Li et al., "Enabling Technology in High-Baud-Rate Coherent Optical Communication Systems," in IEEE Access, vol. 8, pp. 111318-111329, 2020, doi: 10.1109/ACCESS.2020.3003331.

[22] J. -H. Yan, J. -K. Huang, Y. -Y. Lin, J. -W. Hsu and K. -M. Feng, "A MMW Coordinate Multi-Point Transmission System for 5G Mobile Fronthaul Networks based on a Polarization-Tracking-Free PDM-RoF Mechanism," 2020 Optical Fiber Communications Conference and Exhibition (OFC), San Diego, CA, USA, 2020, pp. 1-3.

[23] X. Li, J. Yu and G. -K. Chang, "Photonics-Aided Millimeter-Wave Technologies for Extreme Mobile Broadband Communications in 5G," in Journal of Lightwave Technology, vol. 38, no. 2, pp. 366-378, 15 Jan.15, 2020, doi: 10.1109/JLT.2019.2935137.

[24] K. Mallick et al., "Bidirectional OFDM Based MMW/THzW Over Fiber System for Next Generation Communication," in IEEE Photonics Journal, vol. 13, no. 4, pp. 1-7, Aug. 2021, Art no. 7301207, doi: 10.1109/JPHOT.2021.3104943.

[25] F. Cuesta Quintero, G. Puerto Leguizamón y C. Suárez Fajardo, “Optical partitioning for multicarrier generation in subcarrier multiplexed networks”, INGE CUC, vol. 16, no. 1, 2020. DOI: http://doi.org/10.17981/ingecuc.16.1.2020.013.

[26] ETSI, “5G, NR, Base Station (BS) radio transmission and reception (3GPP TS 38.104 version 15.5.0 Release 15),” 2019. [Online]. Available: https://www.etsi.org/deliver/etsi_ts/138100_138199/138104/15.05.00_60/ts_138104v150500p.pdf